7th EUROMECH Solid Mechanics Conference
J. Ambrósio et.al. (eds.)
Lisbon, Portugal, September 7-11, 2009

FINITE ELEMENT MODELING AND SIMULATION OF DEGENERATION AND HYDROTRACTION THERAPY OF HUMAN LUMBAR SPINE SEGMENTS

László Oroszváry[1], **Márta Kurutz** [2]

[1] Knorr Bremse Hungaria Kft.
1201 Budapest, Helsinki u. 86. Hungary
e-mail: laszlo.oroszvary@knorr.bremse.com

[2] Budapest University of Technology and Economics, Department of Structural Mechanics
1521 Budapest, Műegyetem rkp. 3. Hungary
e-mail: kurutzm@eik.bme.hu

Keywords: Human lumbar functional spinal units, discs, degeneration, hydro-traction therapy, finite element models, numerical simulation.

Abstract. *A large percent of population is affected by low back pain problems all over the world, starting from the degeneration of the lumbar spinal structure, caused generally by ageing and mechanical overloading. If the degeneration is not too advanced, surgical treatments can be avoid, by applying conservative treatments, like traction therapies. Dry traction is a well-known method, however, often happens that instead of the traction effect and stress relaxation, the compression increases in the discs due to muscle activities. This verifies the importance of the suspension hydro-traction therapy, where the muscles are completely relaxed. The aim of this study was doubled: to model and simulate numerically the age-related and accidental degenerations of lumbar functional spinal units (FSU) and to simulate the mechanical answer of the more or less degenerated lumbar segments for the hydro-traction treatment, by using FE method. The basic question was: how to unload the disc to regain or improve its functional and metabolic ability.*

FE simulations of the mechanical behaviour of human lumbar FSUs with life-long age-related and sudden accidental degenerations are presented for tension and compression. Compressive material constants were obtained from the literature, tensional material moduli were determined by parameter identification, using in vivo measured global elongations of segments as control parameters. 3D FE models of a typical FSU of lumbar part L3-S1 were developed extended to several nonlinear and nonsmooth unilateral features of intervertebral discs, ligaments, articular facet joints and attachments. The FE model was validated both for compression and tension, by comparing the numerical calculations with experimental results.

The weightbath hydrotraction therapy decreases pain, increases joint flexibility, and improves the quality of life of patients with cervical or lumbar discopathy. Numerical simulations were investigated to clear the biomechanical effects of hydrotraction treatment of more or less degenerated segments to improve the efficiency of the non-invasive conservative treatment.

1 INTRODUCTION

A large percent of population is affected by low back pain problems all over the world, starting from the degeneration of the lumbar spinal structure, caused generally by normal ageing and mechanical overloading [4]. However, there is a significant correlation between aging and degeneration, distinction has to be drawn between them [5,3]. Degeneration involves both the age-related changes and the specific injurious changes in disc structure, composition and function. In the last three decades FE modeling and simulations have been increasingly applied to spine to examine the mechanical behaviour of healthy or diseased spine and the effects of surgical treatments. There are fewer studies to analyze conservative treatments.

The goal of this study was partly to clear the mechanical backgrounds of the long term age-related degeneration processes and sudden accidental degenerations of intervertebral discs of lumbar FSUs, and partly to clear the mechanical effects of the non-invasive hydrotraction treatment, by using FE numerical simulation. FE analyses are able to simulate details that are difficult to measure experimentally, and which can explain mechanisms in terms of material, geometry or loading.

Intervertebral disc is the most critical component of the spine. The first FE disc models used linear and nonlinear orthotropic materials, assuming homogeneous disc annulus. Later it was modeled as a two-component composite structure, distinguishing the ground substance and the embedded network of collagen fibers. At the same time, the nucleus was modeled as a fluid-like material. Some authors used poroelastic models for the disc. Later FE modeling has been extended to the spinal motion segments, embedding the previously developed disc models into it. To model the complicated geometry of FSU, recently the modern medical image methods CT or MRI are used. FE modeling of FSUs is recently increasing in more and more refined aspects, like disc degeneration.

Dry traction is a well-known method for a long time to treat spinal degenerations, however, often happens that instead of traction effect and stress relaxation, the compression increases in the discs due to muscle activities [6,49,39]. These observations verify the importance of the hydrotraction therapy, a special Hungarian invention, introduced by Moll [31,32], analyzed biomechanically by Bene and Kurutz [8]. During the treatment patients are suspended vertically in water for 20 minutes on a cervical collar or on armpit bars, loaded by extra lead weights applied on the ankles or on a waist-belt. Cervical suspension with ankle loading yields the most effective stretching effect on the lumbar spine, since in this case the contracting effects of muscles stops.

The tensile FE model of FSU has been based on large-scale in vivo measured elongations of human lumbar segments in pure centric tension, during the usual hydro-traction therapy of patients [21,22,25]. Time-dependent elongations of lumbar segments L3-4, L4-5 and L5-S1 were measured, by using an underwater ultrasound measuring method. Based on the measured elongations of segments in terms of biomechanical parameters (age, sex, body height and weight, BMI, spinal level), parameter-dependent viscoelastic general lumbar FSU model L3-S1 have been created for numerical simulation of lumbar FSUs in traction [21,22].

The aim of this study was to simulate numerically the mechanical answer of the healthy and degenerated lumbar FSUs for hydro-traction treatment, by using FE method, considering multiple nonlinearities and nonsmooth characteristics of the mechanical models of FSU. The hydrotraction treatment consists of two separated phases: the beginning instant elastic and the 20 minutes long creeping phase. In this paper only the elastic phase will be analyzed. The basic question was how to unload the disc to regain its metabolic ability in the instant elastic phase of hydrotraction treatment. The numerical simulation of the creeping procedure will be reported later.

2 MODELS, MATERIALS AND METHODS

2.1 Nonlinear and nonsmooth features of FSU

FSU is the smallest unit of the spine, containing all the essential features of the whole spine. It consists of two adjacent vertebrae with the disc between them, and the relating soft tissues like ligaments [49]. FSU has a very complicated mechanical structure with various nonlinear and nonsmooth material structures and unilateral connections. Degenerations make the model even more complicated.

Vertebral bodies are inhomogeneous with high strength cortical cover and viscous internal spongiosa of large ductility and energy absorption capacity [49].

Intervertebral discs are inhomogeneous, strongly viscous, anisotropic, with jellious internal core (nucleus pulposus) and composite fibrous external ring (annulus fibrosus) [49,3]. The external ring is a fiber-like structure with high resistance against compression and smaller for tension. Namely, the layers of a healthy disc annulus are strongly attached in compression, due to the internal support of a healthy nucleus in hydrostatic compression, but they can slope on each other in tension [3]. The internal core of a young healthy disc is a fluid-like jelly material in hydrostatic compression [16,17]. However, during ageing, the nucleus looses its fluid-like features: it changes from fluid to solid material, accompanied by a volume reduction, as well. Consequently, the hydrostatic compression and the internal compressive support of the annulus ring gradually disappears, thus, in compression, the attachment between the annulus layers become weak, they can be separated and can buckle inside the nucleus [3,18].

Ligaments are passive tissues being typical unilateral structures with high resistance for tension and no resistance for compression [49]. They show typical locking-like features: at the beginning of the loading process they have low stiffness, during stretching their resistance increases. Ligaments have anisotropic, fibrous, viscous material, moreover, in certain parts with unilateral attachments to the adjacent bone or disc annulus. In some cases the attachment is strong and bilateral, but in other cases the ligaments and bone or disc are not strongly connected, and contact can occur only if the ligaments are stretched.

The most typical nonsmooth behaviour is manifested by the articular facet joints governing the movements between the adjacent vertebrae. Depending on the type of loading (compression, tension, bending and torsion with their combinations), articular facet joints allow some rotations and deflections between the contacting surfaces, but mainly constrain them in moving [3].

2.2 Loads and displacements in hydrotraction

In cervical suspension three load effects cause traction along the spinal column: the decompressive force as the removal of the compressive body weight existing before the treatment; the active tensile force due to the buoyancy; and the extra lead weights applied to increase the efficiency of the traction effect. The first load is indirect, the second and third loads are direct stretching loads [21]. Figs 1a and 1b illustrates the loads distributed along the spinal column during standing and suspended in water.

The decompressive force F_1 at the lumbar level is about 58-60% of the body weight G, namely, the weight of the head and trunk together, completed by the muscle forces that keep the spine in stable equilibrium in upright standing position. This latter in the lumbar spine is nearly the same as the weight of the upper body [33,42] , thus, $F_1 = 1{,}2G$ can be considered.

The active tensile force F_2 depending on the buoyancy at the lumbar level is: $F_2 = 0{,}46G(1-\rho_w/\rho_b)$, where ρ_w and ρ_b are the densities of water and the human body, re-

spectively [8]. This force is very small, thus, extra lead weight W must be applied, so $F_3 = W(1-\rho_w/\rho_l)$. The sum of these three forces forms the stretching load during the hydrotraction treatment.

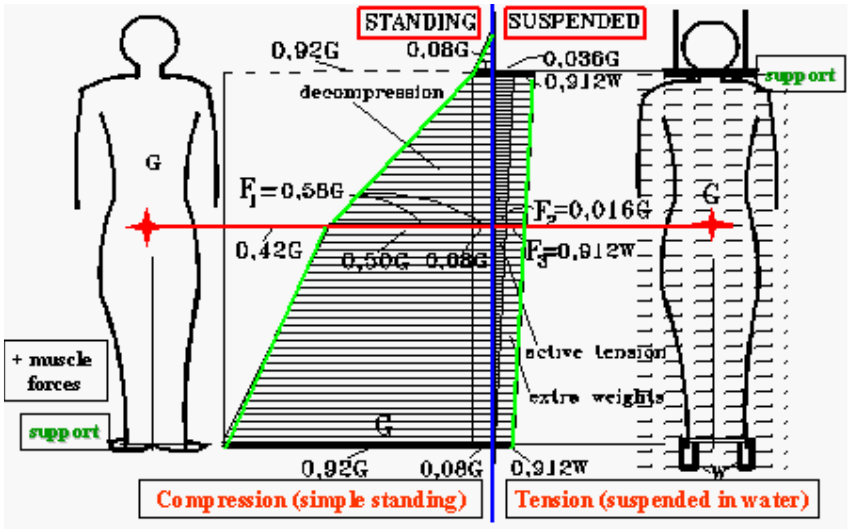

a) b)

Figure 1: Loads on lumbar discs and FSUs in hydrotraction

2.3 Geometric model of FSU

A 3D geometrical model of a typical lumbar motion segment was created (Fig.2a). Geometric data of FSU and its components were obtained by the anatomical measures of a typical lumbar segment.

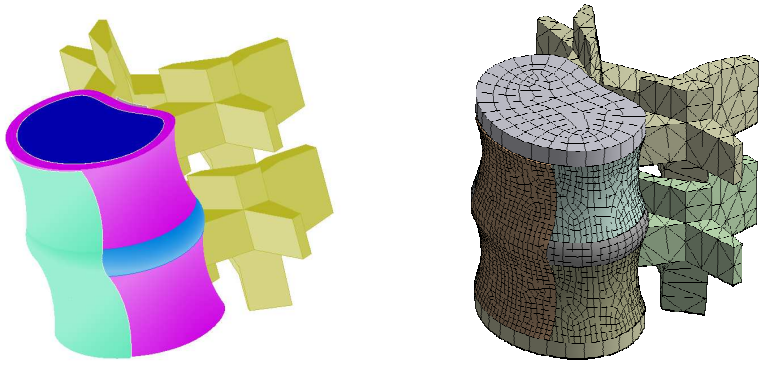

a) b)

Figure 2: Geometric and finite element model of FSU

Cortical and cancellous bone of vertebrae was modeled separately, including the posterior bony elements, too. The thickness of the lateral cortical wall was 0,35 mm, the thickness of the endplates was 0,5 mm. Intervertebral disc was separated to nucleus and annulus. Annulus consists of ground substance and elastic fibers. Annulus matrix was divided to an internal and an external ring [11,12]; and the three layers of annulus fibers were positioned between the nucleus and the internal annulus ring, than between the internal and external annulus rings, finally, around the external annulus. The cross section area of the fibers was 0,1 mm^2. Geometry and orientation of the facet joints were chosen according to the literature [37].

2.4 Finite element model of FSU

The FE mesh was created in three steps. In the first step, the geometrical model of FSU was created by using Pro/Engineer code. In the second step, the FE mesh was generated by ANSYS Workbench, by considering the connections between the several geometrical components as well. Finally the several components were integrated to the FE model by ANSYS Classic. The FE model of the FSU is seen in Fig.2b. The FE model consists of solid, shell and bar elements. Annulus matrix, nucleus, cancellous bone, articular joints and different types of attachments were modeled by Solid_186/187 elements with quadratic displacement behavior. Cortical shells and vertebral end-plates were modeled by Shell_181 elements with four nodes at each element. All ligaments were modeled by Shell_41 elements, with stiffness acting only in tension. The annulus fibers were mapped into Link_10 bar elements with bilinear stiffness matrix resulting in a uniaxial tension-only behaviour.

2.5 Material models of FSU

For the bony elements and endplates we accepted the concerning linear elastic isotropic materials of the literature for both tension and compression [46,15,10,7,9,11,12,40,41,36,50], seen in Table 1.

Components of FSU	Young's moduli [MPa]	Poisson's ratio
Vertebral cortical bone	12000	0,3
Vertebral cancellous bone	150	0,3
Posterior elements, facet	3500	0,3
Endplate	100	0,4
Annulus matrix	4/0,4*	0,45
Annulus fibers	500/400/300**	-
Nucleus	1/0,4*	0,499
Anterior longitud. ligament	8*	0,35
Posterior longitud. ligament	10*	0,35
Other ligaments	5*	0,35

*tension, **external/middle/internal fibers, tension

Table 1: Material moduli of the components of FSU

Annulus ground substance and nucleus were considered linear elastic in compression, and bilinear elastic in tension. In the decompression phase of traction the compressive moduli, while in the active tension phase of traction special tensile moduli were applied. For compression/decompression we used the material constants of the literature, for active tension the Young's moduli of annulus matrix were determined by a parameter identification method based on the in vivo measured global elongations of lumbar FSUs as control parameters [24,26,27], seen in Table 2.

Tensile Young's moduli [MPa]	Male	Female	Total
Young, under 40 years	0,4	0,6	0,5
Middle aged, between 40-60 years	0,8	1,2	1,0
Old, over 60 years	2,8	2,7	2,7
Total	0,8	1,2	1,0

Table 2: Tensile Young's modulus of annulus ground substance obtained by parameter identification

These values were used for the nucleus, as well. For the healthy nucleus, we supposed a fluid-like incompressible material both for tension and compression. The collagen annulus fibers were modeled as linear elastic isotropic tension only materials [46,47,44,45,14,15,28,9].

To simulate the radial variation of type and content of collagen in the fibers, their stiffness was increased outwards [44,29,11,12].

All seven ligaments were integrated in the model, represented by linear elastic tension-only material, using the material data of the literature again (Table 1, [15,51,36]).

2.6 Modeling of age-related long time degenerations

For modeling age-related degeneration five grades were used from healthy (grade 1) to the fully degenerated case (grade 5), seen in Table 3. Degeneration of the disc is manifested in loss of hydration of its components, a drying and stiffening procedure in the texture of both the nucleus and annulus [30,5,3,13], modeled by gradually decreasing Poisson's ratio of nucleus from 0.499 to 0.3, accompanied by increasing Young's modulus from 1 to 81 MPA.

Grades of degeneration		1	2	3	4	5
For compression						
nucleus	Young's modulus	1	3	9	27	81
total	Poisson's ratio	0,499	0,45	0,4	0,35	0,3
annulus	Young's modulus	4	4,5	5	5,5	6
matrix	Poisson's ratio	0,45	0,45	0,45	0,45	0,45
cancelluos	Young's modulus	150	125	100	75	50
bone	Poisson's ratio	0,3	0,3	0,3	0,3	0,3
end-	Young's modulus	100	80	60	40	20
plate	Poisson's ratio	0,4	0,4	0,4	0,4	0,4
For tension						
nucleus	Young's modulus	0,4	1,0	1,6	2,2	2,8
total	Poisson's ratio	0,499	0,45	0,4	0,35	0,3
annulus	Young's modulus	0,4	1,0	1,6	2,2	2,8
matrix	Poisson's ratio	0,45	0,45	0,45	0,45	0,45

Table 3: Modeling of aging degeneration: material moduli from healthy (1) to fully degenerated (5) FSU

At the same time, in the annulus matrix a gradual increase, in the vertebral cancellous bone and endplates a gradual decrease of Young's modulus were considered with aging. The age-related change of the tensile moduli of annulus ground substance and nucleus were modeled by using the results of Table 2.

2.7 Modeling of accidental disc degenerations

In contrast to the aging degeneration, the accidental degenerations occur suddenly, accompanied by disruption, lesions or tears in the annulus or fracture of the endplates [29,34,35], generally due to a mechanical overloading [1].

In this case the hydrostatic compression may suddenly stop in the nucleus, without any stiffening and volume reduction process. These failures can happen in a young disc, as well, or in any age and degeneration phases. This kind of sudden accidental degeneration of nucleus was modeled by decreasing Poisson's ratio of nucleus without increasing Young's modulus.

2.8 Loading cases

The load was distributed along the superior and inferior surface of the upper and lower vertebra, respectively, by applying rigid load distributor plates at both surfaces. For the analysis of age-related degeneration 1000 N, for accidental degeneration 2000 N compression load, for hydrotraction 1000 N indirect and 50 N direct stretching load was applied.

2.9 Validation of the FE models of healthy and degenerated FSU

Validation of the FE models of FSU was performed both in compression and tension. For compression, the distribution of vertical compressive stresses in the mid-sagittal section of the disc obtained by our FE simulation were compared to experimental results of [33,5,3,13,2], obtained by stress profilometry for 2000 N compressive load. The results were in good correspondence with them for both healthy and degenerated FSU. In tension, the calculated elongations of discs were compared to the in vivo measured elongation values of the general lumbar FSU model L3-S1 of [25], giving almost the same results for more or less degenerated discs.

3 RESULTS

3.1 Analysis of long-term adding degeneration

In Figs 3-7 the effect of aging degeneration is illustrated for 1000 N compressive load. Surfaces in Figs a) show the double effect of nucleus hardening and loss of incompressibility during aging. The dotted line indicates the mutual effect of them representing the five age-related degeneration grades in Table 3, illustrated separately in Figs b).

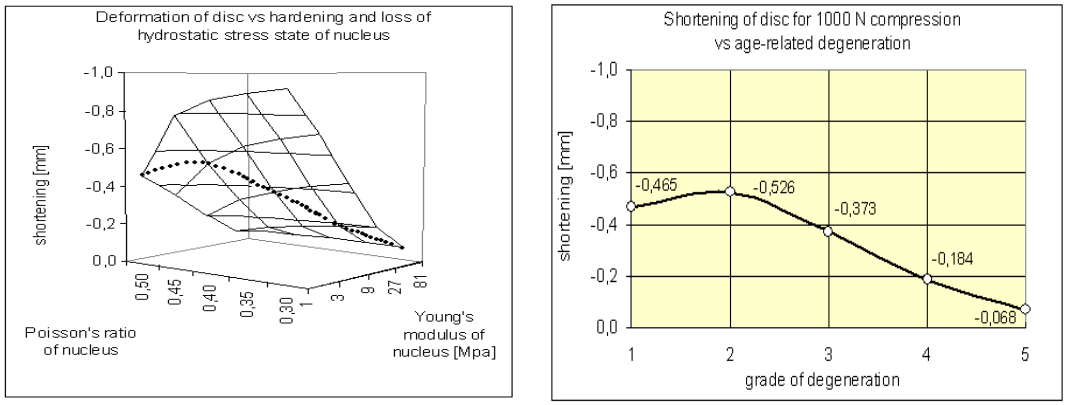

a) b)

Figure 3: Disc shortening for 1000 N compression a) versus separated and mutual effect of nucleus hardening and the loss of hydrostatic state in nucleus, b) versus age-related degeneration

Fig. 3 shows the disc shortening in terms of aging degeneration. The maximum deformability belongs to the mildly degenerated segment. Similar tendency can be seen in Fig. 4 for lateral bulging of disc. Maximum posterior bulging belongs to the healthy and maximum lateral bulging to the mildly degenerated segments.

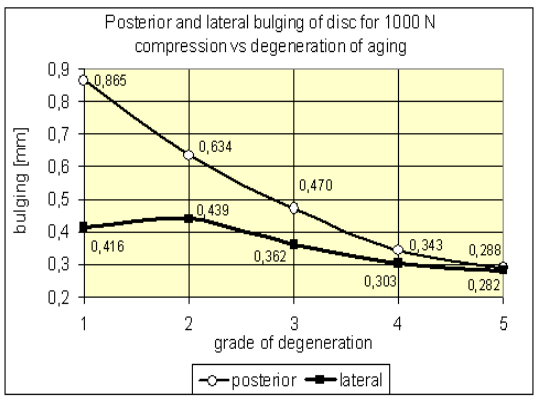

Figure 4: Posterior and lateral bulging for 1000 N compression versus age-related degeneration

Bulging and fiber forces are in correspondence since the diagrams of fiber forces in Fig. 5 show high similarity to the diagrams of bulging and disc deformability in Fig. 4. It can be seen that the loss of hydrostatic compression in nucleus equally increases the disc shortening, bulging and annulus fiber forces; however, nucleus hardening has an inverse effect.

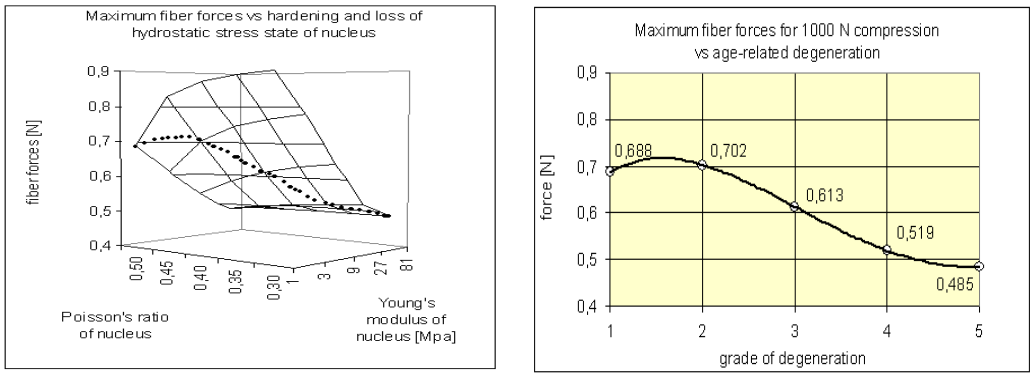

a) b)

Figure 5: Maximum fiber forces for 1000 N compression a) versus separated and mutual effect of nucleus hardening and the loss of hydrostatic state in nucleus, b) versus age-related degeneration

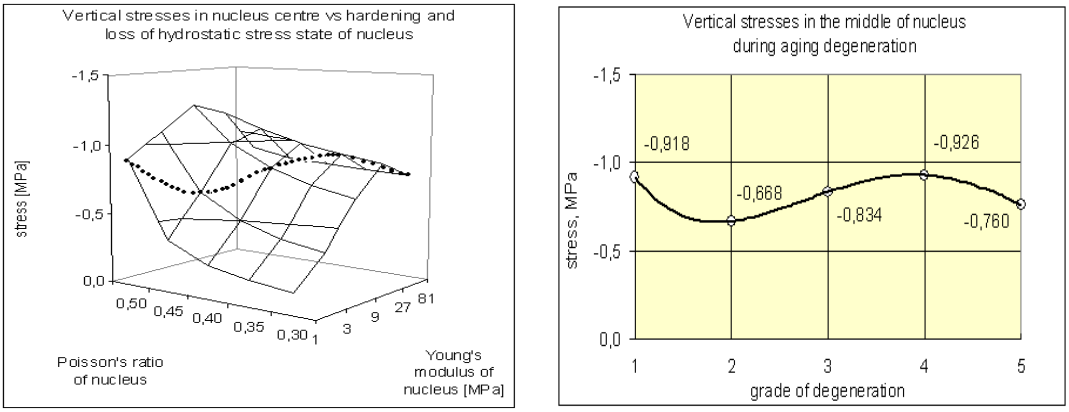

a) b)

Figure 6: Vertical stresses in the middle of nucleus for 1000 N compression a) versus separated and mutual effect of nucleus hardening and the loss of hydrostatic state in nucleus, b) versus age-related degeneration

Figs 6a and 7a show the vertical compressive stresses in the middle of nucleus and in the end of nucleus closed to the annulus, respectively, during aging degeneration, in terms of the loss of hydrostatic compression and nucleus hardening. Figs 6b and 7b shows the change of vertical compressive stresses versus degeneration grades, indicated also in Fig. 6a by dotted line.

3.2 Analysis of sudden accidental degeneration

Fig. 8 illustrates the cases of accidental degeneration of sudden overload of 2000 N compression with a weakened (E=1 MPA) endplate modeling endplate disruption. In Figs 8 the effect of sudden loss of nucleus hydrostatic compression modeling by the decrease of the Poisson's ratio of nucleus is seen when the nucleus quasi bursts out, by constant Young's modulus of nucleus, for young and middle aged nucleus (E=1, 3 and 9 MPa, repectively).

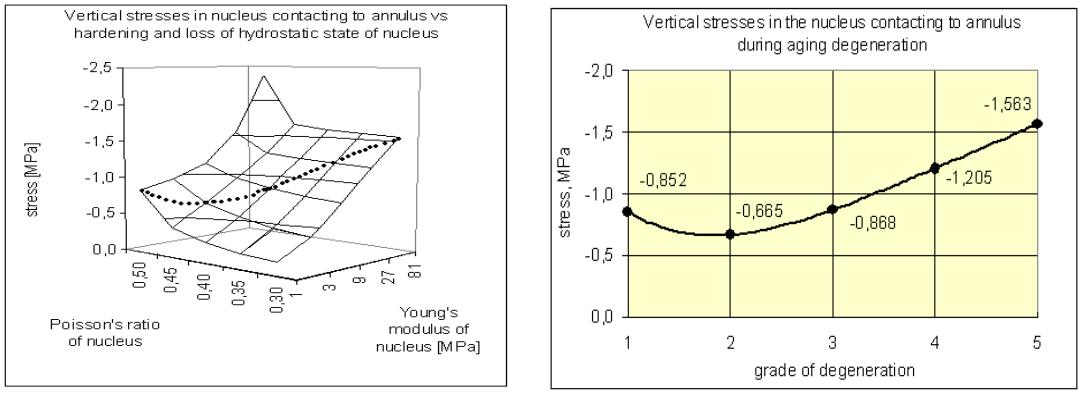

a) b)

Figure 7: Vertical stresses in nucleus contacting to annulus for 1000 N compression a) versus separated and mutual effect of nucleus hardening and the loss of hydrostatic state in nucleus, b) versus age-related degeneration

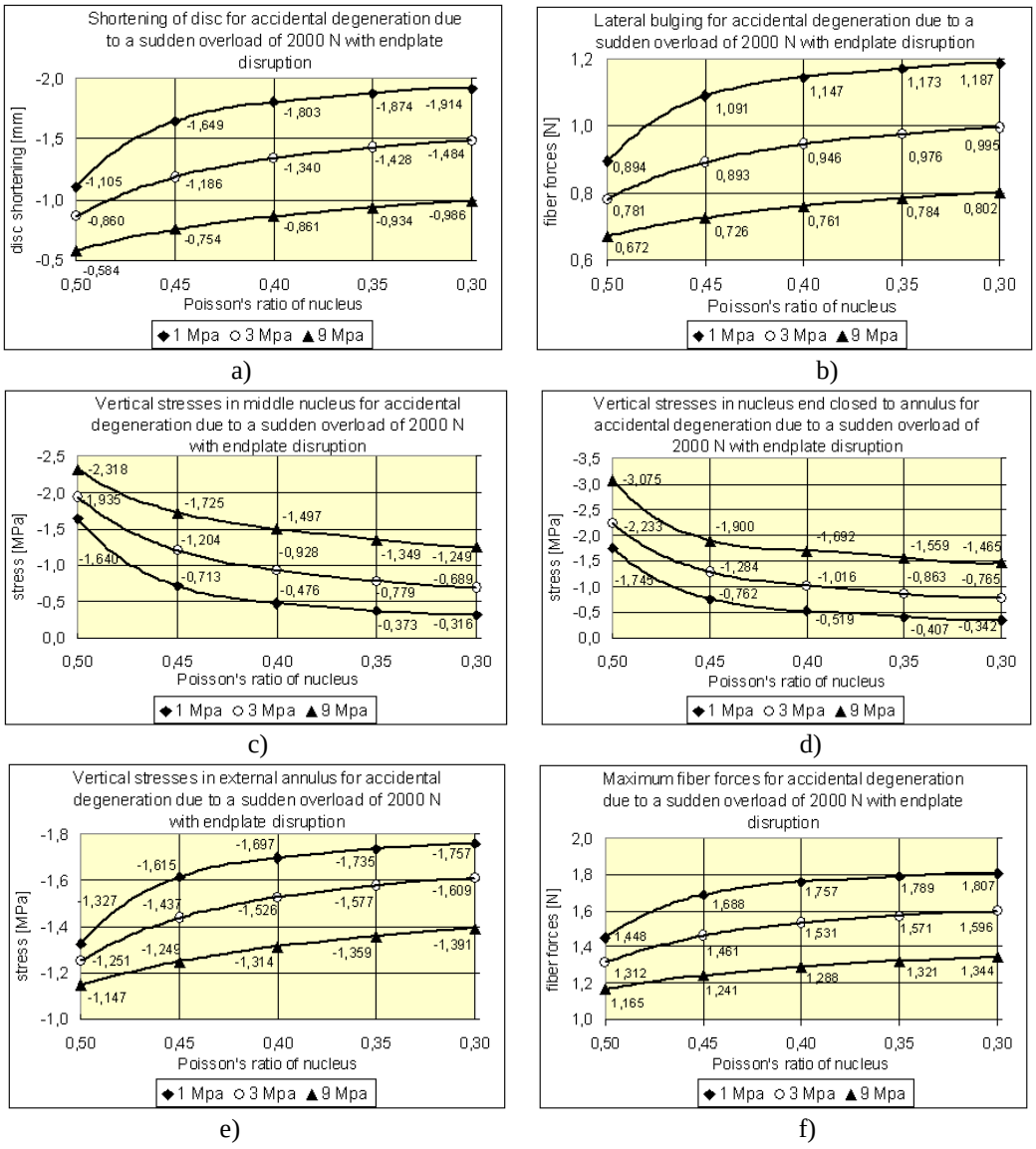

c) d)

e) f)

Figure 8: Effect of accidental degeneration of 2000 N overload with endplate disruption on a) disc shortening, b) lateral buckling, c) maximum annulus fiber forces, d) vertical stresses in the middle of nucleus, e) vertical stresses in the end of nucleus contacting to annulus, f) vertical stresses in the external ring of annulus

It can be seen that the deformability of the disc suddenly increases: disc shortening (Fig. 8a) and bulging (Fig. 8b) equally increase together with the annulus fiber forces (Fig. 8c) with the sudden loss of nucleus incompressibility. Vertical stresses in nucleus middle (Fig. 8d) and in nucleus end (Fig. 8e) decrease while in annulus ring (Fig. 8f) increase during sudden decrease of nucleus compressive load bearing capacity.

3.3 Analysis of hydrotraction therapy

In Fig. 9 the unloading effect of hydrotraction treatment is illustrated in the elastic phase. In Fig. 8a the disc extension, in Fig 8b the unloading of annulus fibers, in Figs 8c and d the unloading of vertical compression of nucleus centre and the border of annulus and nucleus can be seen.

Fig 9a illustrates the extension of disc height at the instant of suspension in the water. It consists of two parts: elongations from the 1000 N decompressive load and from the 50 N active tensile loads. Elongation of discs is specified as an extension compared with the state of disc just before the treatment. That is, zero elongation belongs to the compressed state of segments in normal upright standing position before the treatment.

In Fig. 9b the unloading of tensile forces in annulus fibers are illustrated. The fibers are tension only elements, however, in the active tension state of loading process the annulus fibers share the tensile load bearing with the also tension only ligaments.

Figs 9c and 9d show the vertical stress unloading in nucleus and in nucleus-annulus border respectively, in the instant elastic phase of the treatment, in terms of aging degeneration.

4 DISCUSSION

We modeled the age-related degeneration of FSU in Table 3. Aging type degeneration generally starts in the nucleus. A healthy young nucleus is in a hydrostatic compression state. During aging, the nucleus looses its incompressibility, changes from fluid to a solid-like material accompanied by a hardening process. This kind of nucleus degeneration can be modeled by decreasing Poisson's ratio with increasing Young's modulus [20,19]. Rohlmann et al. [40] distinguished three different grades of disc degeneration, modelling by different loss of disc height and nucleus compressibility, without changing the properties of the annulus. Polikeit et al. [38] classify the grades of disc degeneration as first stiffening of nucleus, than the whole disc, later removing the innermost fiber layers, finally reduction of fiber material properties. We validated our models by experiments both for tension and compression [23].

We can state that the young adults of about 40 years have the most deformable disc. This tendency is even stronger in the viscous period of hydrotraction treatment [22]. Rohlmann et al. [40] concluded that the intersegmental rotations in all physiologic loadings equally increased in mildly and moderately degenerated segments and decreased in severely degenerated segments. We have found the reasons by numerical analysis, by analyzing the separated contrasting effects of decreasing incompressibility and increasing stiffening of nucleus (Figs 3, 5, 6, 7). By loosing the fluid-like properties with decreasing Poisson's ratio, the deformability of the disc increases, and in the contrary, by hardening of nucleus with increasing Young's modulus, the deformability of disc decreases. Thus, during aging, these two contrasting tendencies struggle continuously. In the first period of aging the influence of the loss of hydrostatics is stronger, thus, the maximum of disc deformability occurs about 40-45 years, and later the effect of hardening dominates, so the deformability monotonously decreases (Figs 3, 4). Little et al. [29] state that the hydrostatic load-bearing ability of nucleus has a great importance, thus, the loss of hydrostatic compression in the nucleus has a substantial effect.

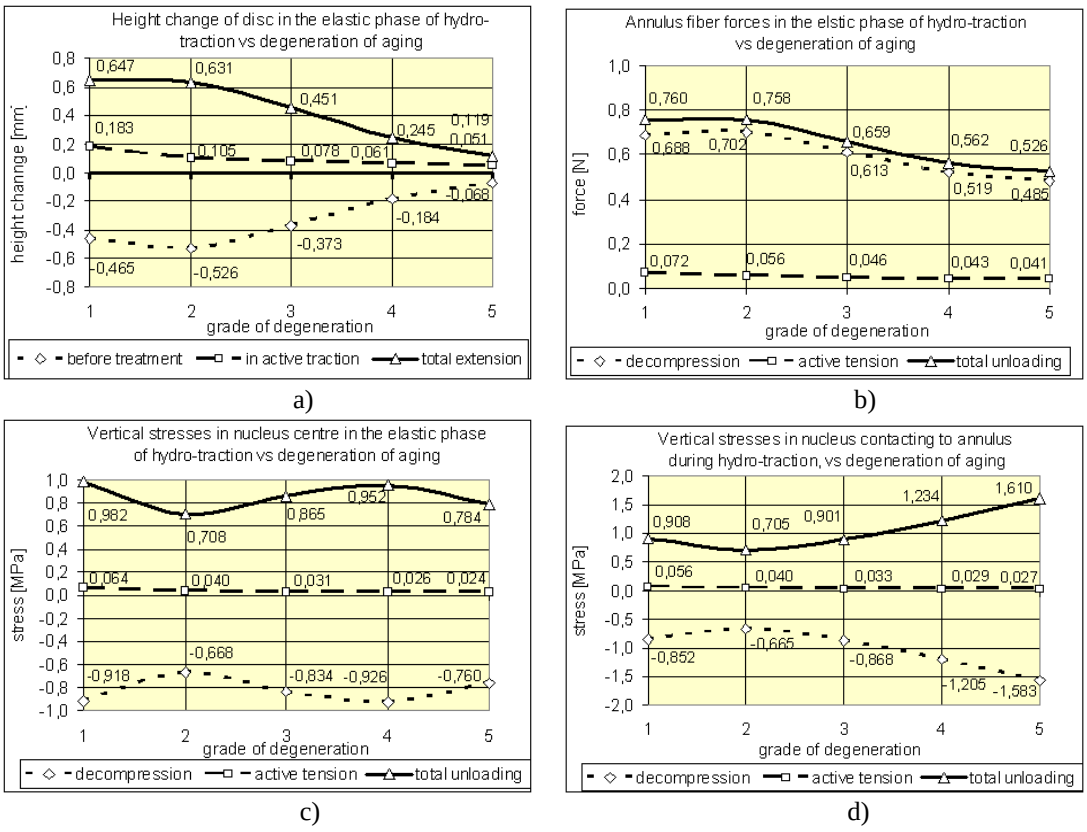

Figure 9: Unloading effect of hydrotraction treatment on a) disc deformation, b) annulus fiber forces, c) vertical compressive stresses in nucleus centre, d) vertical compressive stresses in the border of annulus and nucleus

We can state that the young adults have not only the most deformable, but at the same time the more vulnerable disc. Schmidt et al. [43] proved that the highest internal pressure and strains can be found in healthy and mildly degenerated disc, and with further degeneration they decrease. Therefore the disc prolapse initially increases in the mildly degenerated discs and subsequently decreases in the moderately and severely degenerated discs. Tang et al. [48] concluded that light degeneration of disc leaded to instability of lumbar spine, while the stability restored with further degeneration. The dotted space curve in Fig.5a shows a typical shape of age-related function of maximum fiber forces in nucleus that moves from the lateral part to the posterolateral domain during loading. Inversely, compressive stresses in the nucleus decreased with loss of incompressibility and increased with nucleus hardening (Figs 6 and 7). Indeed, the stiffness of both the nucleus and the annulus is minimum about the age of 40-45 years, thus the risk of instability is maximum in this life period. Later, the effect of nucleus hardening dominates, thus, the deformability decreases and the nucleus load bearing increases.

The effect of accidental nucleus damage, namely the sudden stop of hydrostatic compression state due to a 2000 N overload with endplate disruption is seen in Fig. 8. In this case, when the nucleus quasi bursts out, the overall resistance of the segment decreases and the height of disc radically decreases (by 73, 72 and 6973% for E=1, 3, 9 MPa, respectively, Fig. 8a), accompanied by the radical increase of disc bulging (lateral, by 33, 27 and 19% for E=1, 3, 9 MPa, respectively, Fig 8b). At the same time, the vertical stresses decrease in the nucleus centre (by 81, 64 and 46% for E=1, 3, 9 MPa, respectively, Fig. 8c) and decrease in the nucleus edge contacting to the annulus (by so does the slight decrease in annulus around the nucleus (by 80, 66, 52% for E=1, 3, 9 MPa, respectively, Fig. 8d) and increase in the external

annulus (by 32, 29 and 21% for E=1, 3, 9 MPa, respectively, Fig. 8e). The forces in the suddenly overloaded annular fibers increase (by 25, 22 and 15% for E=1, 3, 9 MPa, respectively, Fig. 6f). Thus the annular fiber forces become extremely large, by considering the 0,1 mm^2 cross sectional area of them, the tensile stress in them increase from 14,5 to 18,1, from 13,1 to 16,0 and from 11,7 to 13,4 MPa in the case of E=1, 3, 9 MPa of nucleus, respectively. This sudden overload yields annulus disruption and other degenerations of disc.

The unloading effect of hydrotraction therapy is seen in Fig. 9. The beneficial impact of weight-bath therapy lays mainly on the unloading of the compressed discs. However, nobody knows the original intact (zero) state of the disc, fibers and other components of FSU, every state of them is relative. Thus, we started from the compressed state before the treatment, this state was considered as zero state. So, in Figs 9 the state variables are distinguished: caused by 1000 N decompression load and 50 N active stretching loads. These two components of elastic disc extensions are seen in Fig 9a with the sum of them as total extension.

The disc extension is accompanied by unloading of disc bulging, consisting of also the decompressive and active tensile components. While in young age the posterior contraction is about the double of that of the anterior ones due to the straightening of lumbar curvature of a flexible young spine; in old age the anterior and posterior contractions are equally smaller. These contractions help to unload the nerves around the spinal canal from the overloading compression that causes low back pain. Consequently, this contractive nerve unloading is one of the main aims of traction therapies.

The annular fibers are tension only elements that share the tensile load bearing with the tension only ligaments in the active tensile state of loading process (Fig. 8b). During active tensile period, the direction of the fibers change, the slope of them increases.

Figs 9c and 9d illustrates the stress unloading of nucleus during hydrotraction treatment, in comparison with the compressed state of segment before the treatment. Thus, here the unloading tensile stresses are seen due to the decompressive and active tensile load. Also in stress unloading, the dominating effect is the decompression, partly due to the large decompressive load and very small active tensile load and partly due to the bilinear elastic behaviour of disc annulus and nucleus (Table 3).

5 CONCLUSION

Based on the results of FE simulation of hydrotraction therapy of more or less degenerated lumbar spine segments, the following conclusions can be drawn.

The ageing degeneration of FSU can be modeled by variation of the Young's modulus and Poisson's ratio of nucleus accompanied with changing stiffness of annulus matrix, end-plates and cancellous bone. The tensile Young’s moduli of annulus and nucleus can be smaller than the compressive ones. The healthy and degenerating models have been validated by experimental results both for tension and compression.

The aging degeneration of nucleus reduces the axial deformability and bulging of disc, and additionally, reduces the bending stresses in end-plates. It also reduces the tension in annulus fibers, but causes high vertical compressive stress peaks in nucleus-annulus border. The loss of hydrostatic compression state in nucleus has a crucial role in the deformability of the disc. This effect explains that the low back pain problems insult so frequently the young adults, their discs are more deformable and more vulnerable at the same time.

The mechanical evidences, the deformation and stress unloading effects of hydrotraction therapy have been proved numerically to support the medical experiences of improving functional and metabolic ability of segments and decreasing low back pain problems.

6 ACKNOWLEDGEMENTS

The present study was supported by the project OTKA T-033020, T-046755, K-075018. The authors are grateful to A. Kutrik for the help in FE modelling the FSU.

REFERENCES

[1] Acaroglu, E.R., Iatridis, J.C., Setton, L.A., Foster, R.J., Mow, V.C., Weidenbaum, M., 1995. Degeneration and aging affect the tensile behaviour of human lumbar anulus fibrosus, Spine, 20(24), 2690-2701.

[2] Adams, M.A., Dolan, P., 2005. Spine biomechanics, *Journal of Biomechanics*, 38(10), 1972-1983.

[3] Adams, M.A., Bogduk, N., Burton, K., Dolan, P., 2002. The Biomechanics of Back Pain, Churchill Livingstone, Edinburgh, London, New York, Oxford, Philadelphia, St Louis, Sydney, Toronto, 238 p.

[4] Adams, M.A., Freeman, B.J., Morrison, H.P., Nelson, I.W., Dolan, P., 2000, Mechanical initiation of intervertebral disc degeneration, *Spine*, 25(13), 1625-1636.

[5] Adams, M.A., McNally, D.S., Dolan, P., 1996. Stress distributions inside intervertebral discs. The effects of age and degeneration. J. Bone Joint Surg. Br. 78 (6), 965-972.

[6] Andersson, G.B., Schultz, A.B., Nachemson, A.L., 1983. Intervertebral disc pressures during traction, Scand. J. Rehabil. Med. Suppl. 9, 88-91.

[7] Antosik, T., Awrejcewicz, J., 1999. Numerical and experimental analysis of biomechanics of three lumbar vertebrae, Journal of .Theoretical and Applied Mechanics, 3, 37.

[8] Bene É., Kurutz, M., 1993. Weight-bath and its biomechanics, *(in Hungarian), Orvosi Hetilap, 134. 21.* 1123-1129.

[9] Cheung, J.T.M., Zhang, M., Chow, D.H.K., 2003. Biomechanical responses of the intervertebral joints to static and vibrational loading: a finite element study, Clinical Biomechnaics, 18, 790-799.

[10] Ciach, M., Awrejcewicz, J., 2000. Finite element analysis and experimental investigations of the intervertebral discs in the human lumbar and cervical spine and porcine lumbar spinal segment, Computer Assisted Mechanics and Engineering Sciences, 7, 91-101.Denoziere, G., 2004. Numerical modeling of ligamentous lumbar motion segment, Master thesis, Georgia Institute of Technology, 2004.

[11] Denoziere, G., 2004. Numerical modeling of ligamentous lumbar motion segment, Master thesis, Georgia Institute of Technology, 2004.

[12] Denoziere, G., Ku, D.N., 2006. Biomechanical comparison between fusion of two vertebrae and implantation of an artificial intervertebral disc, Journal of Biomechanics, 39, 766-775.

[13] Dolan, P., Adams, M.A., 2001. Recent advances in lumbar spinal mechanics and their significance for l, Clinical Biomecanics., 16, Suppl.(1), S8-S16.

[14] Fagan, M.J., Julian, S., Siddall, D.J., Mohsen, A.M., 2002b. Patient specific spine models. Part 1: finite element analysis of the lumbar intervertebral disc – a material sensitiv-

ity study, Proceedings of the Institution of Mechanical Engineers, Part H: 216(5), 299-314.

[15] Goel, V.K., Monroe, B.T., Gilbertson, L.G., Brinckmann, P., 1995. Interlaminar shear stresses and laminae separation in the disc. Finite element analysis of the L3-L4 motion segment subjected to axial compressive loads. Spine, 20(6), 689-698.

[16] Iatridis, J.C., Wedenbaum, M., Setton, L.A., Mow, V.C., 1996. Is the nucleus pulposus a solid or a fluid? Mechanical behaviours of the nucleus pulposus of the human intervertebral disc, Spine, 21(10), 1174-1184.

[17] Iatridis, J.C., Setton, L.A., Wedenbaum, M., Mow, V.C., 1997. Alterations in the mechanical behavior of the human lumbar nucleus pulposus with degeneration and aging. Journal of Orthopaedic Research, 15(2), 318-322.

[18] Iatridis, J.C., Setton, L.A., Foster, R.J., Rawlins, B.A., Weidenbaum, M., Mow, V.C., 1998. Degeneration affects the anisotropic and nonlinear behaviours of human anulus fibrosus in compression, Journal of Biomechanics, 31(6), 535-544.

[19] Kim, Y.E., Goel, V.K., Weinstein, J.N., Lim, T.H., 1991. Effect of disc degeneration at one level on the adjacent level in axial mode, Spine, 16, 331-335.

[20] Kurowski, P., Kubo, A., 1986. The relationship of degeneration of the intervertebral disc to mechanical loading conditions on lumbar vertebrae, Spine, 11, 726-731.

[21] Kurutz, M., 2006a. Age-sensitivity of time-related in vivo deformability of human lumbar motion segments and discs in pure centric tension, Journal of Biomechanics, 39(1), 147-157.

[22] Kurutz, M., 2006b. In vivo age- and sex-related creep of human lumbar motion segments and discs in pure centric tension, Journal of Biomechanics, *39*(7), 1180-9.

[23] Kurutz, M., Oroszváry, L., 2009. Finite element modelling and simulation of hydrotraction treatment of lumbar spine segments in elastic phase, Journal of Biomechanics (submitted).

[24] Kurutz, M., Tornyos, Á., 2004. Numerical simulation and parameter identification of human lumbar spine segments in traction, In: Bojtár I. (ed.): Proc. of the First Hungarian Conference on Biomechanics, ISBN 963 420 799 5, pp. 254-263, Budapest, Hungary, June 10-11, 2004.

[25] Kurutz, M., Bene É., Lovas, A., 2003. In vivo deformability of human lumbar spine segments in pure centric tension, measured during traction bath therapy, Acta of Bioengineering and Biomechanics, 5(1), 67-92.

[26] Kurutz, M., Bene, É., Lovas, A., Molnár, P., Monori, E., 2002a. In vivo biomechanical experiments for measuring traction deformations of human lumbar spine during weight-bath therapy. (In Hung.), Orvosi Hetilap, 143 (13), 673-684.

[27] Kurutz, M., Lovas, A., Tornyos, Á., Molnár P., Monori, E., 2002b. Experimental biomechanical tensile model of human lumbar spine segments in vivo, In: Mang, H.A., Rammerstorfer, F.G., Eberhardsteiner, J. (eds.): Long papers of 5th World Congress on Computational Mechanics, July 7-12, 2002, Vienna, Austria, pp. 1-10.

[28] Lavaste, F., Skalli, W., Robin, S., Roy-Camille, R., Mazel, C., 1992. Three-dimensional geometrical and mechanical modelling of lumbar spine, Journal of Biomechanics, *25*(10), 1153-1164.

[29] Little, J.P., Adam, C.J., Evans, J.H., Pettet, G.J., Pearcy, M.J., 2007. Nonlinear finite element analysis of anular lesions in the L4/5 intervertebral disc, Journal of Biomechanics, 40, 2744-2751.

[30] Mcnally, D.S., Adams, M.A., 1992. Internal intervertebral disc mechanics as revealed by stress profilometry, Spine, 17, 66-73.

[31] Moll, K., 1956. Die Behandlung der Discushernien mit den sogenannten "Gewichtsbadern", Contempl. Rheum., 97, 326-329.

[32] Moll, K., 1963. The role of traction therapy in the rehabilitation of discopathy, Rheum. Balneol. Allerg., 3, 174-177.

[33] Nachemson, A.L., 1981. Disc pressure measurements, Spine, 6(1), 93-97.

[34] Natarajan, R.N., Williams, J.R., Andersson, G.B., 2004. Recent advances in analytical modelling of lumbar disc degeneration. Spine, 29, 2733-2741.

[35] Natarajan, R.N., Williams, J.R., Andersson, G.B., 2006. Modeling changes in intervertebral disc mechanics with degeneration, Journal of Bone and Joint Surgery Am. 88(4), Suppl. 2:36-40.

[36] Noailly, J., Wilke, H.J., Planell, J.A., Lacroix, D., 2007. How does the geometry affect the internal biomechanics of a lumbar spine bi-segment finite element model? Consequences on the validation process, Journal of Biomechanics, 40, 2414-2425.

[37] Panjabi, M.M., Oxland, T., Takata, K., Goel, V., Duranceau, J., Krag, M., 1993. Articular facets of the human spine, quantitative three dimensional anatomy, Spine, 18, 1298-1310.

[38] Polikeit, A., Nolte, L.P., Ferguson, S.J., 2004. Simulated influence of osteoporosis and disc degeneration on the load transfer in a lumbar functional spinal unit, Journal of Biomechanics, 37, 1061-1069.

[39] Ramos, G., Martin, W., 1994. Effects of vertebral axial decompression on intradiscal pressure, Journal of Neurosurgery. 81(3), 350-353.

[40] Rohlmann, A., Zander, T., Schmidt, H., Wilke, H.J., Bergmenn, G., 2006a. Analysis of the influence of disc degeneration on the mechanical behaviour of a lumbar motion segment using the finite element method, Journal of Biomechanics, 39, 2484-2490.

[41] Rohlmann, A., Bauer, L., Zander, T., Bergmann, G., Wilke, H.J., 2006b. Determination of trunk muscle forces for flexion and extension by using a validated finite element model of the lumbar spine and measured in vivo data, Journal of Biomechanics, 39, 981-989.

[42] Sato, K., Kikuchi, S., Yonezawa, T., 1999, In vivo intradiscal pressure measurement in healthy individuals and in patients with ongoing back problems, Spine, 24(23), 2468-2474.

[43] Schmidt, H., Kettler, A., Rohlmann, A., Claes, L., Wilke, H,J.. 2007. The risk of disc prolapses with complex loading in different degrees of disc degeneration - a finite element analysis, Clinical Biomechanics, 22(9), 988-998.

[44] Shirazi-Adl, A., 1989a. On the fibre composite material models of the annulus – comparison of predicted stresses. Journal of Biomechanics, 22, 357-365.

[45] Shirazi-Adl, A., 1989b. Strain in fibers of a lumbar disc. Analysis of the role of lifting in producing disc prolapse, Spine, 14(1), 96-103.

[46] Shirazi-Adl, S.A., Shrivastava, S.C., Ahmed, A.M., 1984. Stress analysis of the lumbar disc-body unit in compression. A three-dimensional nonlinear finite element study, Spine, 9(2), 120-34.

[47] Spilker, R.L. Jakobs, D.M., Schultz, A.B., 1986. Material constants for a finite element model of the intervertebral disc with a fibre composite annulus, Journal of Biomechanical Engineering, 108, 1-11.

[48] Tang, X.J., Chen, Q.X., Liu, Y.S., Li, F.C., 2008. Analysis of lumbar disc degeneration using three-dimensional nonlinear finite element method, (Article in Chinese), Zhonghua Yi Xue Za Zhi, 88(23), 1634-1638.

[49] White, A. A., Panjabi, M. M., 1990. *Clinical Biomechanics of the Spine*, Lippincott Williams and Wilkins, Philadelphia, etc.

[50] Williams, J.R., Natarajan, R.N., Andersson, G.B.J., 2007. Inclusion of regional poroelastic material properties better predicts biomechanical behaviour of lumbar discs subjected to dynamic loading, Journal of Biomechanics, 40, 1981-1987.

[51] Zander, T., Rohlmann, A., Bergmann, G., 2004. Influence of ligament stiffness on the mechanical behaviour of a functional spinal unit, Journal of Biomechanics, 37, 1107-1111.